International Journal of Solids and Structures 50 (2013) 687–698

Contents lists available at SciVerse ScienceDirect

International Journal of Solids and Structures

journal homepage: www.elsevier.com/locate/ijsolstr

Analytical solutions of two-layer beams with interlayer slip and bi-linear interface law

Francesca Campi, Ilaria Monetto *

DICCA – Department of Civil, Chemical and Environmental Engineering, University of Genoa, Via Montallegro 1, 16145 Genova, Italy

ARTICLE INFO

Article history:
Received 17 May 2012
Received in revised form 30 October 2012
Available online 28 November 2012

Keywords:
Two-layer beam
Interlayer slip
Nonlinear interface

ABSTRACT

A new formulation to analyze two-layer beams with interlayer slip is proposed. Each layer is modeled as a linearly elastic Timoshenko beam. The connection between the layers is assumed to be perfect in the transverse direction while imperfect in the longitudinal one (only interlayer slips are allowed). The interface behavior in the longitudinal direction is described through a linear non proportional relationship relating tangential reactions transmitted between the two layers and slips. The problem is then solved analytically and a novel closed form solution is obtained. Explicit expressions for all static and kinematic variables are derived. This analytical solution is shown to be employed in the analysis of composite beams for different boundary and loading conditions generating interfacial tractions that induce an irreversible process of progressive debonding at the interface. Some numerical examples are considered and a parametric analysis performed to investigate the influence of the interface behavior on the response of the composite beam when the layers are still elastic.

1. Introduction

Two-layer beams consist of the association of two layers, having the same or different thickness and width and made of the same or different materials, bonded together by appropriate mechanical devices or adhesive joints. Steel–concrete or timber–concrete beams, beams or columns reinforced with steel plates or fiber composite stripes are some examples. Typically, the resulting composite structural elements show enhanced performances in both global stiffness and strength compared to those obtained by the sum of individual layers without connection.

A perfect connection that retains any relative displacement between the layers would allow a complete transmission of both normal and shear stresses and ensure an optimal performance of the joint. However, in practice, connections exhibit finite stiffness, so that relative transverse and longitudinal displacements (respectively, uplifts and slips) at the interface between the layers can occur. In practice, only imperfect connections ensuring a partial composite action can be obtained. As an example, mechanical shear devices, such as nails or steel studs, retain interlayer uplifts but allow interlayer slips; on the contrary, both slips and uplifts can occur in adhesive joints depending on the thickness of the adhesive interlayer. Moreover, flaws and defects due, for instance, to manufacturing errors can easily form at the interfaces. Under loading conditions that generate interlayer stresses these flaws may propagate starting a process of progressive debonding at the interface. This leads to a further reduction of the stiffness of the connection and, as a consequence, of the global stiffness and strength of the composite beam, when the layers are still elastic.

The interface between layers then represents a weak element in composite beams. The optimal design of such structural elements depends not only on the geometrical and mechanical properties of the single layers, but also on the optimal design of the joint between the layers. The investigation of the effects of the interfacial behavior on the mechanical response of composite systems is then of great importance. In order to do this, even simplified models which provide explicit analytical solutions are preferable to numerical analyses usually performed for prescribed geometry, material properties and interface constitutive behavior.

The problem of two-layer beams with imperfect connection has been the object of a large number of studies in literature. The first partial composite action theory was proposed by Newmark et al. (1951) to analyze steel–concrete beams with mechanical shear connectors. Their theory is based on the assumptions that no uplifts between the layers are possible and plane sections remain plane during the loading process. The layers were modeled as linearly elastic Euler–Bernoulli beams and the connection was treated as a continuous distribution of longitudinal springs characterized by a linearly elastic constitutive law. The analytical solution for a simply supported beam subjected to a concentrated transverse load was derived.

Since the pioneering work of Newmark, other models were offered which differ in one or more assumptions. Girhammar and

* Corresponding author. Tel.: +39 010 353 2951; fax: +39 010 353 2534.
E-mail address: ilaria.monetto@unige.it (I. Monetto).

0020-7683/$ - see front matter © 2012 Elsevier Ltd. All rights reserved.
http://dx.doi.org/10.1016/j.ijsolstr.2012.10.032

Gopu (1993) and Girhammar and Pan (2007) compared exact first and second order analyses and focused on the magnification in the internal forces and displacements due to the second order effects. Cosenza and Mazzolani (1993) found further closed-form solutions for simply supported beams subjected to different loading conditions. More recently, effects of shear deformation were included in the original theory modeling the layers as Timoshenko beams. Schnabl et al. (2007) described the solution procedure of the equations governing the model and presented a parametric study to investigate the influence of shear deformation on the response of simply supported two-layer beams subjected to uniformly distributed loads. Xu and Wu (2007) obtained analytical solutions of the problem for uniformly distributed loads and different boundary conditions. Finally, Adekola (1968) first extended Newmark's model to imperfect interfaces not only in the longitudinal direction but also in the transverse direction (both slips and uplifts can occur). He solved the differential equations governing the problem by finite differences; then Robinson and Naraine (1988) and Gara et al. (2006) proposed alternative numerical procedures of solution in order to handle beams with a wider class of loading and boundary conditions. Only more recently, explicit analytical solutions were presented in the framework of both linearly elastic Euler–Bernoulli (Wang, 2006; Kroflič et al., 2010) and Timoshenko beam theories (Wang and Qiao, 2004; Bennati et al., 2009).

Experimental evidences show that, also for moderate levels of slip, joints exhibit nonlinear behavior corresponding to a process of progressive debonding (see e.g., Ollgaard et al., 1971; McCutcheon, 1986; Chajes et al., 1996; Manfredi et al., 1999; Planinc et al., 2008). In a lot of works the nonlinear behavior of the interface and/or of the layer materials are taken into account. However, since this complicates the equations governing the problem, most works deal with specific problems and employ numerical procedures of solution. There is a lack of analytical solutions with general validity that can be employed to investigate the influence of nonlinearity on the response of composite beams. Wheat and Calixto (1994) considered interface nonlinearity and proposed an energy formulation that, because of its complexity, permits one to obtain explicit expressions for some variables only. Wang (2006) presented an analytical study of debonding at the interface induced by a flexural crack in a FRP-plated concrete beam. He modeled the reinforced beam as two linearly elastic Euler–Bernoulli beams bonded together through an interface characterized by a linearly elastic normal stress-uplift law in the transverse direction and a nonlinear shear stress-slip law in the longitudinal direction. Namely, as a good approximation of this nonlinear relationship, a bi-linear shear stress-slip law was considered. Closed-form solutions were obtained for the interfacial shear and normal stresses and the deflection of the beam in each stage of the debonding process. More recently, Foraboschi (2009) developed a nonlinear analytical model for two-layer beams with interlayer slip and bi-linear interface law. The mathematical model, related boundary conditions and exact solution were presented for a simply supported beam subjected to uniformly distributed loads and for a specific choice of bi-linear interface law. Namely, elasto-softening and, as particular case, elasto-plastic interfaces were considered.

In this paper a novel analytical solution of the problem of partial interaction in two-layer beams is presented. The formulation followed is based on standard assumptions already made in some previous theories: (i) small strains, displacements and rotations; (ii) layers modeled as linearly elastic Timoshenko beams; (iii) bond between the layers modeled as perfect interface in the transverse direction (no uplifts are possible) and as imperfect interface in the longitudinal direction (slips can occur). Namely, a linear non proportional law relating interfacial shear tractions and slips is chosen to describe the interfacial behavior. On one hand, this choice permits one to analytically solve the problem, the main goal of the present paper; on the other, it describes suitably different regimes the interface can experience during a loading process (not only elastic, perfectly plastic or softening but also hardening interfacial behavior, depending on the value of suitable coefficients). Some experimental evidences showed that connections realized by means of mechanical shear devices can exhibit behaviors more suitably described by elasto-hardening than elasto-plastic or softening interface laws (McCutcheon, 1986; Planinc et al., 2008). The novelty in our formulation is that explicit expressions having general validity independently of the interface regime for all static and kinematic variables of the problem are derived. Furthermore, this fundamental solution can be employed in the analysis of two-layer beams with interlayer slip and nonlinear interfacial behavior for different boundary and loading conditions. In order to do this, nonlinear interfacial behavior can be conveniently approximated through a multi-linear law, so that for each linear branch the fundamental solution is valid. This choice is supported by the comparison of experimental and numerical studies and was previously made by many authors working on the subject as well as on similar problems (Schreyer and Peffer, 2000; Lu et al., 2005; Wang, 2006). The novel fundamental solution presented in this paper can then be employed to solve a wider class of problems (beams with different loading and boundary conditions, as well as different interface constitutive laws) than those analyzed in all previous similar works on two-layer beams with elastic layers and interlayer slip. Such previous similar works can be reproduced as particular cases by setting suitably the model parameters.

The aim of this work is to study the effect of interface nonlinearity on the structural response of the composite structure with a view towards an optimal design of the joint. As an example, a two-layer cantilever beam with different bi-linear interface laws and subjected to a load at the free end is considered. A parametric analysis is then performed to investigate the influence of the parameters that characterize the interface constitutive relationship on the response of the composite beam. As a consequence of the assumptions made, the analysis is restricted to composite beams with layers connected through nails, studs or sufficiently thin adhesive interlayers for which uplifts can be neglected. It is straightforward that the case of normal separation at the interface is much more involved. Introducing nonlinearity of the layer materials complicates further the formulation. Analytical solutions are difficult to obtain with the exception of considering convenient multi-linear approximations also for the constitutive laws of layer materials, so that the fundamental solution is still valid.

The paper is organized as follows. Section 2 deals with the equilibrium, compatibility and constitutive equations governing the proposed formulation and presents their rearrangement to two coupled linear differential equations for shear and normal interfacial tractions. Details of the solution procedure leading to exact expressions of interfacial tractions are described in Section 3. Subsequent derivation of all other static and kinematic variables is then shown in Section 4. Section 5 lays out the procedure for obtaining all the arbitrary constants contained in the general solution of the problem. Finally, in addition to verifying the new formulation, Section 6 shows a practical application to the analysis of a two-layer cantilever beam during a process of progressive debonding at the interface. The results of the parametric analysis performed are also discussed. Section 7 concludes the paper with a final discussion of the advances in understanding the mechanical response of two-layer beams with interlayer slip.

2. Model formulation

The composite beam under consideration consists of two layers having constant cross sections and made of linearly elastic and

homogeneous materials. The layers are connected by a continuous bond assumed to be perfect in the transverse direction, while to ensure a partial composite action in the longitudinal direction. As a consequence, interlayer slips can occur at the interface, but no separation or interpenetration between the layers is possible.

Under the assumption of small strains, displacements and rotations, each layer is modeled as a linearly elastic Timoshenko beam. The connection is modeled by continuously distributed normal and tangential reactions, the latter related to interlayer slips according to a suitable relationship approximating the typically nonlinear interfacial behavior.

With reference to Fig. 1, under the assumption that cross sections remain plane after deformation, the displacement components of a generic point at level y in the ith layer, say s_{zi} in the longitudinal direction and s_{yi} in the transverse direction, yield:

$$s_{zi} = u_i + (y - y_i)\varphi_i, \quad s_{yi} = w_i, \tag{1}$$

where: u_i and w_i are, respectively, the axial displacement and deflection of points along the axis and φ_i is the rotation of the cross section of the ith layer ($i = 1,2$); y_i represents the level of the axis of the ith layer. The relative displacements in the longitudinal and transverse directions at the interface between the layers, say respectively Δs_t (interlayer slip) and Δs_n (uplift), then follow:

$$\begin{aligned} \Delta s_t &= \bar{s}_{z2} - \bar{s}_{z1} = u_2 - h_2\varphi_2 - u_1 - h_1\varphi_1 \\ \Delta s_n &= \bar{s}_{y2} - \bar{s}_{y1} = w_2 - w_1, \end{aligned} \tag{2}$$

where: $\bar{s}_{zi}$, $\bar{s}_{yi}$ are the displacement components of the points in the ith layer ($i = 1,2$) along the interface between the layers; h_i measures the distance between the interface and the axis of the ith layer. Furthermore, according to Timoshenko beam theory, taking into account the effects of shear deformation, the compatibility equations for the two layers ($i = 1,2$) are:

$$\varepsilon_i = u_i', \quad \gamma_i = \varphi_i + w_i', \quad \chi_i = \varphi_i', \tag{3}$$

where: primes denote differentiation with respect to z; ε_i, γ_i and χ_i are, respectively, the axial deformation, shear strain and curvature of the ith layer.

Considering now the free-body diagram shown in Fig. 2, the equilibrium equations for the two layers are:

$$\begin{aligned} &N_i' = (2i-3)p_t - q_{zi}, \quad Q_i' = (2i-3)p_n - q_{yi}, \quad M_i' \\ &\quad = Q_i - h_i p_t - m_i, \end{aligned} \tag{4}$$

where: q_{zi}, q_{yi} and m_i are uniformly distributed loads applied to the ith layer ($i = 1,2$); N_i, Q_i and M_i are, respectively, the axial and shear forces and the bending moment in the ith layer; p_t and p_n are, respectively, the shear and normal tractions at the interface between the layers. Then, differentiating the third of Eq. (4) and substituting the result in the second of Eq. (4) gives:

$$M_i'' = (2i-3)p_n - h_i p_t' - q_{yi}. \tag{5}$$

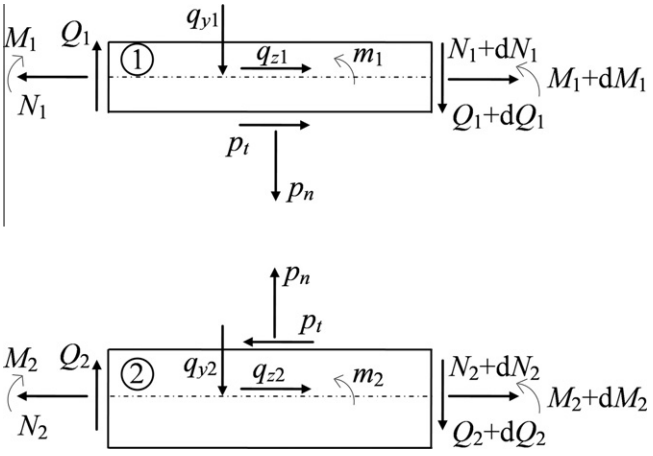

Fig. 2. Free-body diagram of an infinitesimal beam element.

Being both layers made of linearly elastic materials, the constitutive equations assume the form:

$$N_i = K_{\varepsilon i}\varepsilon_i, \quad Q_i = K_{\gamma i}\gamma_i, \quad M_i = K_{\chi i}\chi_i, \tag{6}$$

with $i = 1,2$; $K_{\varepsilon i}$, $K_{\gamma i}$ and $K_{\chi i}$ are, respectively, the axial, shear and bending stiffnesses of the ith layer ($i = 1,2$).

Now, substituting the compatibility conditions (3) in the constitutive Eq. (6) and the result in the equilibrium Eqs. (4) and (5) gives the following system of six differential equations for the eight unknowns u_i, w_i, φ_i ($i = 1,2$) and p_t, p_n:

$$\begin{aligned} &u_i'' = K_{\varepsilon i}^{-1}[(2i-3)p_t - q_{zi}], \\ &\varphi_i' + w_i'' = K_{\gamma i}^{-1}[(2i-3)p_n - q_{yi}], \\ &\varphi_i''' = K_{\chi i}^{-1}\left[(2i-3)p_n - h_i p_t' - q_{yi}\right]. \end{aligned} \tag{7}$$

Such basic equations, together with the bond conditions at the interface, govern the problem of the equilibrium of two-layer beams. Firstly, the assumption of perfect connection in the transverse direction y imposes that:

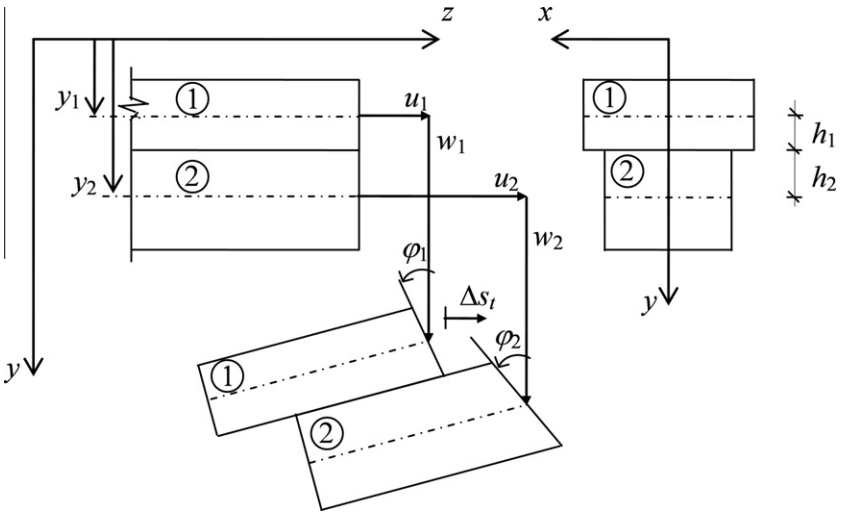

Fig. 1. Geometry and typical deformed configuration assumed in the present model.

$$\Delta s_n = w_2 - w_1 = 0, \tag{8}$$

from which it follows that the two layers undergo equal deflections:

$$w_1 = w_2 = w. \tag{9}$$

Secondly, the partial composite action in the longitudinal direction z is assumed to be described through the following linear relationship between the shear tractions and the interlayer slips at the interface (Fig. 3a):

$$p_t = A\Delta s_t + B = A(u_2 - u_1 - h_1\varphi_1 - h_2\varphi_2) + B, \tag{10}$$

with A and B coefficients. It is worthwhile observing that the choice of such a simple linear interface constitutive law makes possible the derivation of analytical solutions of the problem, the main goal of the present paper. Furthermore, different values of the coefficients A and B describe different types of interfacial regime within a multi-linear approximated description of the nonlinear interface behavior. As an example, Table 1 summarizes the values of the coefficients A and B related to the exemplary bi-linear interfacial regimes shown in Fig. 3b.

In order to solve the problem under consideration, it is convenient to rearrange the above Eqs. (7), (8) and (10), as detailed in what follows. First, differentiate Eq. (8) four times with respect to z; then, insert the second of Eq. (7), differentiated twice, and the third of Eq. (7) in the result to finally obtain:

$$\left(K_{\gamma 1}^{-1} + K_{\gamma 2}^{-1}\right)p_n'' - \left(K_{\chi 1}^{-1} + K_{\chi 2}^{-1}\right)p_n + \left(K_{\chi 2}^{-1}h_2 - K_{\chi 1}^{-1}h_1\right)p_t' = q_n, \tag{11}$$

having defined

$$q_n = K_{\chi 1}^{-1}q_{y1} - K_{\chi 2}^{-1}q_{y2}. \tag{12}$$

Analogously, differentiate Eq. (10) three times with respect to z; then, insert the first of Eq. (7), differentiated once, and the third of Eq. (7) in the result to finally obtain:

$$\begin{aligned} &p_t''' - A\left(K_{\varepsilon 1}^{-1} + K_{\varepsilon 2}^{-1} + K_{\chi 1}^{-1}h_1^2 + K_{\chi 2}^{-1}h_2^2\right)p_t' \\ &\quad + A\left(K_{\chi 2}^{-1}h_2 - K_{\chi 1}^{-1}h_1\right)p_n \\ &\quad = q_t, \end{aligned} \tag{13}$$

having defined

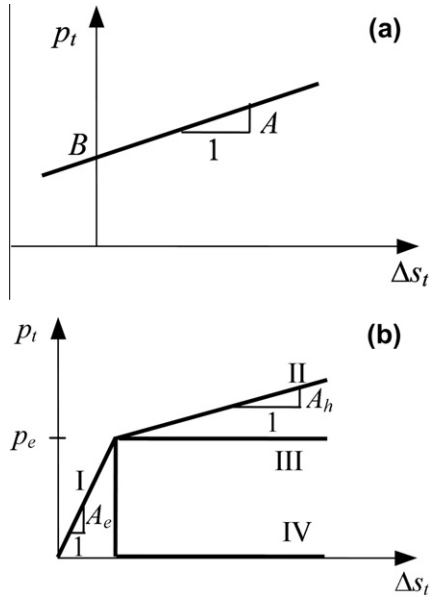

Fig. 3. Interface laws: (a) linear; (b) bi-linear.

Table 1
Coefficients A and B in Eq. (10) for interfacial regimes shown in Fig. 3b.

Interfacial regime	Elastic I	Hardening II	Perfectly-plastic III	Debonded IV
A	$A_e > 0$	$A_h > 0$	0	0
B	0	$p_e(1 - A_h/A_e)$	p_e	0

$$q_t = A\left(K_{\chi 1}^{-1}h_1 q_{y1} + K_{\chi 2}^{-1}h_2 q_{y2}\right). \tag{14}$$

Eqs. (11) and (13) together with the constants defined in Eqs. (12) and (14) are two coupled linear differential equations with constant coefficients for the two unknowns p_t and p_n. Details of the solution procedure leading to exact expressions of the shear and normal interfacial tractions are described in Section 3. Subsequent derivation of all other static and kinematic variables through the remaining equations governing the problem is then detailed in Section 4. Finally, Section 5 deals with the strategy to obtain all the arbitrary constants contained in such general solution.

For the special case of elastic interface a verification of Eqs. (11) and (13) can be found in Schnabl et al. (2007) and Xu and Wu (2007). In both papers governing equations were rearranged and two coupled differential equations of higher order in the interlayer slip and normal traction (Schnabl et al., 2007) or in the deflection and rotation (Xu and Wu, 2007) were obtained.

Finally, under the assumption of infinite shear stiffness of the layers ($K_{\gamma i} \to \infty$, $i = 1,2$) Eq. (11) simplifies to a first order differential equation. Such simplified equation together with Eq. (13) can be proved to govern the problem of two-layer beams with interlayer slip according to classical Euler–Bernoulli beam theory, for which the effects of shear deformation are neglected. For the special case of elastic interface this simplified model reduces exactly to that first proposed by Newmark. More details are discussed in Appendix A.

3. Interfacial tractions

In the case of particular composite beams consisting of two layers having geometry and material properties satisfying the condition:

$$K_{\chi 2}^{-1}h_2 - K_{\chi 1}^{-1}h_1 = 0, \tag{15}$$

the solution of Eqs. (11) and (13) is straightforward, since the two differential equations become uncoupled and assume the simplified forms:

$$p_n'' - \left(K_{\gamma 1}^{-1} + K_{\gamma 2}^{-1}\right)^{-1}\left(K_{\chi 1}^{-1} + K_{\chi 2}^{-1}\right)p_n = \left(K_{\gamma 1}^{-1} + K_{\gamma 2}^{-1}\right)^{-1}q_n, \tag{16}$$

$$p_t''' - A\left(K_{\varepsilon 1}^{-1} + K_{\varepsilon 2}^{-1} + K_{\chi 1}^{-1}h_1^2 + K_{\chi 2}^{-1}h_2^2\right)p_t' = q_t, \tag{17}$$

with q_n and q_t given by (12) and (14), respectively. Eq. (16) is a second order linear differential equation with constant coefficients whose general solution can be given as:

$$p_n = C_1\cosh(\alpha z) + C_2\sinh(\alpha z) + \bar{p}_n, \tag{18}$$

where:

$$\begin{aligned} &\alpha = \sqrt{\left(K_{\gamma 1}^{-1} + K_{\gamma 2}^{-1}\right)^{-1}\left(K_{\chi 1}^{-1} + K_{\chi 2}^{-1}\right)} \quad \text{and} \quad \bar{p}_n \\ &\quad = \left(K_{\chi 1}^{-1} + K_{\chi 2}^{-1}\right)^{-1}\left(K_{\chi 2}^{-1}q_{y2} - K_{\chi 1}^{-1}q_{y1}\right), \end{aligned} \tag{19}$$

with C_j ($j = 1,2$) two arbitrary constants. Analogously, Eq. (17) is a third order linear differential equation with constant coefficients whose general solution contains three other arbitrary constants, say C_j ($j = 3,\ldots,5$). This general solution can assume three different

forms depending on the value of the coefficient A, that is on the regime experienced by the interface:

$$p_t = \begin{cases} \frac{1}{2}C_3 z^2 + C_4 z + C_5 & \text{for } A = 0 \ (q_t = 0) \\ C_3 + C_4\cosh(\beta z) + C_5\sinh(\beta z) + \bar{p}_t z & \text{for } A > 0 \\ C_3 + C_4\cos(\beta z) + C_5\sin(\beta z) + \bar{p}_t z & \text{for } A < 0 \end{cases} \tag{20}$$

having defined

$$\beta = \sqrt{|A|\left(K_{\varepsilon 1}^{-1} + K_{\varepsilon 2}^{-1} + K_{\chi 1}^{-1}h_1^2 + K_{\chi 2}^{-1}h_2^2\right)} \quad \text{and} \quad \bar{p}_t = -\frac{K_{\chi 1}^{-1}h_1 q_{y1} + K_{\chi 2}^{-1}h_2 q_{y2}}{K_{\varepsilon 1}^{-1} + K_{\varepsilon 2}^{-1} + K_{\chi 1}^{-1}h_1^2 + K_{\chi 2}^{-1}h_2^2}. \tag{21}$$

In the general case of composite beams that do not satisfy condition (15), the solution of the coupled differential problem requires a rearrangement of the governing Eqs. (11) and (13). In order to do that, Eq. (11) is solved for the first derivative of the interfacial shear tractions:

$$p_t' = \left(K_{\chi 1}^{-1}h_1 - K_{\chi 2}^{-1}h_2\right)^{-1}\left[\left(K_{\gamma 1}^{-1} + K_{\gamma 2}^{-1}\right)p_n'' - \left(K_{\chi 1}^{-1} + K_{\chi 2}^{-1}\right)p_n - q_n\right], \tag{22}$$

which, substituted in Eq. (13), leads to a fourth order linear differential equation with constant coefficients for the interfacial normal tractions that can be written as:

$$p_n'''' + \hat{a}p_n'' + \hat{b}p_n = \hat{c}, \tag{23}$$

where:

$$\hat{a} = -\left[\left(K_{\chi 1}^{-1} + K_{\chi 2}^{-1}\right)\left(K_{\gamma 1}^{-1} + K_{\gamma 2}^{-1}\right)^{-1} + A\left(K_{\varepsilon 1}^{-1} + K_{\varepsilon 2}^{-1} + K_{\chi 1}^{-1}h_1^2 + K_{\chi 2}^{-1}h_2^2\right)\right], \tag{24}$$

$$\hat{b} = A\left(K_{\gamma 1}^{-1} + K_{\gamma 2}^{-1}\right)^{-1}\left[\left(K_{\chi 1}^{-1} + K_{\chi 2}^{-1}\right)\left(K_{\varepsilon 1}^{-1} + K_{\varepsilon 2}^{-1}\right) + K_{\chi 1}^{-1}K_{\chi 2}^{-1}(h_1 + h_2)^2\right], \tag{25}$$

$$\hat{c} = \left(K_{\gamma 1}^{-1} + K_{\gamma 2}^{-1}\right)^{-1}\left[q_t\left(K_{\chi 1}^{-1}h_1 - K_{\chi 2}^{-1}h_2\right) - q_n A\left(K_{\varepsilon 1}^{-1} + K_{\varepsilon 2}^{-1} + K_{\chi 1}^{-1}h_1^2 + K_{\chi 2}^{-1}h_2^2\right)\right], \tag{26}$$

with q_n and q_t given by (12) and (14). It is straightforward that constant coefficients in Eq. (23) can either vanish or be positive or negative depending on the interfacial regime, as well as on the geometry and material properties of the layers. As a consequence, the general solution of the differential equation can be written in different forms.

Case 1. For $\hat{b} = 0$ ($A = 0$ then $q_t = 0$, $\hat{c} = 0$ and $\hat{a} < 0$), the general solution for normal tractions yields:

$$p_n = C_1 + C_2 z + C_3\cosh(\alpha z) + C_4\sinh(\alpha z), \tag{27}$$

having defined

$$\alpha = \sqrt{-\hat{a}}. \tag{28}$$

Case 2. For $\hat{b} \neq 0$ and $\hat{a} = 0$ ($A < 0$ then $\hat{b} < 0$), the general solution of Eq. (23) yields:

$$p_n = C_1\cosh(\alpha z) + C_2\sinh(\alpha z) + C_3\cos(\alpha z) + C_4\sin(\alpha z) + \bar{p}_n, \tag{29}$$

having introduced

$$\alpha = \sqrt[4]{-\hat{b}} \quad \text{and} \quad \bar{p}_n = \hat{c}/\hat{b}, \tag{30}$$

with $\hat{b}$ and $\hat{c}$ given by (25) and (26).

Case 3. In the most general case, $\hat{b} \neq 0$ and $\hat{a} \neq 0$, the solution of Eq. (23) is more complicated and can assume five different forms:

$$p_n = \begin{cases} C_1\cosh(\alpha_1 z) + C_2\sinh(\alpha_1 z) + C_3\cosh(\alpha_2 z) + C_4\sinh(\alpha_2 z) + \bar{p}_n & \text{for } \hat{a} < 0 \\ C_1\cos(\alpha_1 z) + C_2\sin(\alpha_1 z) + C_3\cos(\alpha_2 z) + C_4\sin(\alpha_2 z) + \bar{p}_n & \text{for } \hat{a} > 0 \end{cases} D > 0$$

$$\begin{cases} (C_1 + C_2 z)\cosh(\alpha_1 z) + (C_3 + C_4 z)\sinh(\alpha_1 z) + \bar{p}_n & \text{for } \hat{a} < 0 \\ (C_1 + C_2 z)\cos(\alpha_1 z) + (C_3 + C_4 z)\sin(\alpha_1 z) + \bar{p}_n & \text{for } \hat{a} > 0 \end{cases} D = 0,$$

$$\begin{cases} C_1\cosh(\alpha_4 z)\cos(\alpha_3 z) + C_2\cosh(\alpha_4 z)\sin(\alpha_3 z) + C_3\sinh(\alpha_4 z)\cos(\alpha_3 z) + C_4\sinh(\alpha_4 z)\sin(\alpha_3 z) + \bar{p}_n & \text{for } \hat{a} < 0 \\ C_1\cosh(\alpha_3 z)\cos(\alpha_4 z) + C_2\cosh(\alpha_3 z)\sin(\alpha_4 z) + C_3\sinh(\alpha_3 z)\cos(\alpha_4 z) + C_4\sinh(\alpha_3 z)\sin(\alpha_4 z) + \bar{p}_n & \text{for } \hat{a} > 0 \end{cases} D < 0 \tag{31}$$

where

$$D = \hat{a}^2/4 - \hat{b}, \tag{32}$$

$$\alpha_1 = \sqrt{|\frac{\hat{a}}{2} - \sqrt{D}|}, \quad \alpha_2 = \sqrt{|\frac{\hat{a}}{2} + \sqrt{D}|}, \quad \alpha_3 = \frac{1}{2}\sqrt{2\sqrt{\hat{b}} - |\hat{a}|}, \quad \alpha_4 = \frac{1}{2}\sqrt{2\sqrt{\hat{b}} + |\hat{a}|}, \tag{33}$$

whereas $\bar{p}_n$ is defined by the second of Eq. (30).

Finally, when the interfacial normal tractions have been obtained, Eq. (22) can be simply integrated to obtain the interfacial shear tractions. Their general analytical expression contains one more arbitrary constant, say C_5, and can be written as:

$$p_t = \left(K_{\chi 1}^{-1}h_1 - K_{\chi 2}^{-1}h_2\right)^{-1}\left[\left(K_{\gamma 1}^{-1} + K_{\gamma 2}^{-1}\right)p_n' - \left(K_{\chi 1}^{-1} + K_{\chi 2}^{-1}\right)\int p_n dz - q_n z\right] + C_5, \tag{34}$$

with q_n given by Eq. (12) and $\int \cdot dz$ denoting integration with respect to z.

4. Internal forces and displacements

When the interfacial normal and shear tractions have been obtained, the sets of Eqs. (2), (3), (4) and (6) can be simply solved to derive closed form expressions for all the remaining unknowns (internal forces and displacements), as detailed in what follows.

Integration of the first and second of Eq. (4) gives the axial and shear forces in both layers (i = 1,2):

$$N_i = (2i-3)\int p_t dz - q_{zi}z + C_{5+i}, \quad Q_i = (2i-3)\int p_n dz - q_{yi}z + C_{7+i}, \tag{35a}$$

whereas, taking into account the second of Eq. (35a), integration of the third of Eq. (4) gives the bending moments in the layers:

$$M_i = (2i-3)\int\int p_n \mathrm{d}z - h_i \int p_t \mathrm{d}z - q_{yi}\frac{z^2}{2} - m_i z + C_{7+i} z + C_{9+i}, \tag{35b}$$

where for brevity, hereinafter, $\int\int \cdot \mathrm{d}z$ indicates integration of $\cdot$ twice with respect to z. As a consequence of such integrations, Eq. (35) contain six other arbitrary constants C_j ($j = 6,\ldots,11$).

Through the (algebraic) constitutive Eq. (6), the axial deformation, shear strain and curvature of both layers can now be straightforwardly obtained. The result is then employed to derive analytical expressions of the axial displacements, deflections and rotations, respectively, through further integration of the compatibility Eq. (3). Immediately the axial displacements and the rotations are obtained ($i = 1,2$):

$$u_i = K_{\varepsilon i}^{-1}\left[(2i-3)\int\int p_t \mathrm{d}z - q_{zi}\frac{z^2}{2} + C_{5+i} z\right] + C_{11+i}, \tag{36a}$$

$$\varphi_i = K_{\chi i}^{-1}\left[(2i-3)\int\int\int p_n \mathrm{d}z - h_i \int\int p_t \mathrm{d}z - q_{yi}\frac{z^3}{6} + (C_{7+i} - m_i)\frac{z^2}{2} + C_{9+i} z\right] + C_{13+i}, \tag{36b}$$

where for brevity, hereinafter, $\int\int\int \cdot \mathrm{d}z$ indicates integration of $\cdot$ three times with respect to z. Then, on the basis of Eq. (36b), the deflections follow:

$$w_i = \begin{cases} (3-2i)K_{\chi i}^{-1}\int\int\int\int p_n \mathrm{d}z + (2i-3)K_{\gamma i}^{-1}\int\int p_n \mathrm{d}z \\ \quad + K_{\chi i}^{-1} h_i \int\int\int p_t \mathrm{d}z + K_{\chi i}^{-1}\left[q_{yi}\frac{z^4}{24} + (m_i - C_{7+i})\frac{z^3}{6} - C_{9+i}\frac{z^2}{2}\right], \\ \quad - K_{\gamma i}^{-1}\left(q_{yi}\frac{z^2}{2} - C_{7+i} z\right) - C_{13+i} z + C_{15+i} \end{cases} \tag{36c}$$

where for brevity, hereinafter, $\int\int\int\int \cdot \mathrm{d}z$ indicates integration of $\cdot$ four times with respect to z. In Eqs. (36) C_j ($j = 12,\ldots,17$) are six other arbitrary constants.

Finally, from Eq. (2) the displacement discontinuities between the layers yield:

$$\Delta s_t = \begin{cases} \left(K_{\chi 1}^{-1} h_1 - K_{\chi 2}^{-1} h_2\right)\int\int\int p_n \mathrm{d}z + \left(K_{\varepsilon 1}^{-1} + K_{\varepsilon 2}^{-1} + K_{\chi 1}^{-1} h_1^2 + K_{\chi 2}^{-1} h_2^2\right)\int\int p_t \mathrm{d}z \\ \quad + \left[K_{\chi 1}^{-1} h_1 q_{y1} + K_{\chi 2}^{-1} h_2 q_{y2}\right]\frac{z^3}{6} + \left[K_{\chi 1}^{-1} h_1 (m_1 - C_8) + K_{\chi 2}^{-1} h_2 (m_2 - C_9)\right]\frac{z^2}{2}, \\ \quad + \left[K_{\varepsilon 1}^{-1} q_{z1} - K_{\varepsilon 2}^{-1} q_{z2}\right]\frac{z^2}{2} + \left[K_{\varepsilon 2}^{-1} C_7 - K_{\varepsilon 1}^{-1} C_6 - K_{\chi 1}^{-1} h_1 C_{10} - K_{\chi 2}^{-1} h_2 C_{11}\right] z \\ \quad - C_{12} + C_{13} - h_1 C_{14} - h_2 C_{15} \end{cases} \tag{37a}$$

$$\Delta s_n = \begin{cases} -\left(K_{\chi 1}^{-1} + K_{\chi 2}^{-1}\right)\int\int\int\int p_n \mathrm{d}z + \left(K_{\gamma 1}^{-1} + K_{\gamma 2}^{-1}\right)\int\int p_n \mathrm{d}z + \left(K_{\chi 2}^{-1} h_2 - K_{\chi 1}^{-1} h_1\right)\int\int\int p_t \mathrm{d}z \\ \quad + \left[K_{\chi 2}^{-1} q_{y2} - K_{\chi 1}^{-1} q_{y1}\right]\frac{z^4}{24} + \left[K_{\chi 2}^{-1}(m_2 - C_9) - K_{\chi 1}^{-1}(m_1 - C_8)\right]\frac{z^3}{6} - C_{16} + C_{17} \\ \quad + \left[K_{\chi 1}^{-1} C_{10} - K_{\chi 2}^{-1} C_{11} + K_{\gamma 1}^{-1} q_{y1} - K_{\gamma 2}^{-1} q_{y2}\right]\frac{z^2}{2} + \left[K_{\gamma 2}^{-1} C_9 - K_{\gamma 1}^{-1} C_8 + C_{14} - C_{15}\right] z \end{cases} \tag{37b}$$

To sum up, the general solution of the problem of equilibrium of two-layer beams with interlayer slip contains 17 arbitrary constants to be determined by imposing 17 conditions. The procedure followed is analogous to that worked out by Bennati et al. (2009), as described in Section 5.

5. Arbitrary constants

In order to evaluate the 17 arbitrary constants contained in the general solution of the problem of equilibrium of two-layer beams with interlayer slip, a segment of composite beam having length L_r whose all points along the interface ($0 \leqslant z \leqslant L_r$) behave accordingly to a particular regime, denoted by the subscript "r", is considered.

The prescription of boundary conditions at both ends $z = 0$ and $z = L_r$ of the segment under consideration gives only 5 + 5 conditions. The kinematic or corresponding static quantities on which such conditions can be imposed are w, φ_1, φ_2, u_1, u_2 or, alternatively, $Q = Q_1 + Q_2$, M_1, M_2, N_1, N_2. The first boundary condition on w or, alternatively, on the resultant shear Q follows from the assumption of perfect connection in the transverse direction so that the two layers undergo equal deflections.

Seven further conditions need to be imposed. They are obtained by imposing that the expressions (37) found for the displacement discontinuities satisfy the bond conditions Eq. (8) of perfect connection in the transverse direction and Eq. (10) of partial connection in the longitudinal direction for all points of the interface. This results in seven relations among the arbitrary constants that depend on the interface regime under consideration, as well as on the geometry and material properties of the layers.

As an example, the determination of these conditions is now illustrated in the special case of composite beams having geometry and material properties satisfying Eq. (15). In this case, from Eqs. (37), each displacement discontinuity between the layers depends only on the interfacial tractions acting along the same direction. So, substituting the general solution (18) for p_n, integrated twice and four times with respect to z, in Eq. (37b), on the basis of definitions (19), the displacement discontinuity Δs_n assumes the explicit form:

$$\begin{aligned} \Delta s_n = {} & \left[K_{\chi 2}^{-1}(m_2 - C_9) - K_{\chi 1}^{-1}(m_1 - C_8)\right]\frac{z^3}{6} \\ & + \left[K_{\gamma 2}^{-1} C_9 - K_{\gamma 1}^{-1} C_8 + C_{14} - C_{15}\right] z - C_{16} + C_{17} \\ & + \left[\left(K_{\chi 1}^{-1} + K_{\chi 2}^{-1}\right)^{-1}\left(K_{\gamma 1}^{-1} K_{\chi 2}^{-1} - K_{\gamma 2}^{-1} K_{\chi 1}^{-1}\right)(q_{y1} + q_{y2}) + K_{\chi 1}^{-1} C_{10}\right. \\ & \left. - K_{\chi 2}^{-1} C_{11}\right]\frac{z^2}{2}, \end{aligned} \tag{38}$$

which satisfies the bond condition (8) for any $0 \leqslant z \leqslant L_r$ if and only if:

$$\begin{aligned} & K_{\chi 2}^{-1}(m_2 - C_9) - K_{\chi 1}^{-1}(m_1 - C_8) = 0, \quad C_{16} = C_{17}, \\ & K_{\gamma 2}^{-1} C_9 - K_{\gamma 1}^{-1} C_8 + C_{14} - C_{15} = 0, \\ & \left(K_{\chi 1}^{-1} + K_{\chi 2}^{-1}\right)^{-1}\left(K_{\gamma 1}^{-1} K_{\chi 2}^{-1} - K_{\gamma 2}^{-1} K_{\chi 1}^{-1}\right)(q_{y1} + q_{y2}) \\ & \quad + K_{\chi 1}^{-1} C_{10} - K_{\chi 2}^{-1} C_{11} = 0. \end{aligned} \tag{39}$$

which represent four algebraic relations among the arbitrary constants. Analogously, further relations are obtained by imposing that the condition (10) of imperfect connection in the longitudinal direction is satisfied. However, since the general solution for p_t depends on both geometry and material properties of the layers and on the interfacial regime under consideration, two cases are considered.

In the general case of $A \neq 0$, the same procedure adopted for the transverse direction is followed. The general solution (20) for p_t, integrated twice with respect to z, is substituted in Eq. (37a) to derive an explicit expression for Δs_t that, introduced in the condition (10) gives:

$$\begin{aligned} & A\left[C_3\left(K_{\varepsilon 1}^{-1} + K_{\varepsilon 2}^{-1} + K_{\chi 1}^{-1} h_1^2 + K_{\chi 2}^{-1} h_2^2\right) + K_{\chi 1}^{-1} h_1 (m_1 - C_8)\right. \\ & \quad \left. + K_{\chi 2}^{-1} h_2 (m_2 - C_9)\right]\frac{z^2}{2} \\ & \quad + A\left[K_{\varepsilon 1}^{-1} q_{z1} - K_{\varepsilon 2}^{-1} q_{z2}\right]\frac{z^2}{2} \\ & \quad + \left[(K_{\chi 1}^{-1} h_1 q_{y1} + K_{\chi 2}^{-1} h_2 q_{y2})\left(K_{\varepsilon 1}^{-1} + K_{\varepsilon 2}^{-1} + K_{\chi 1}^{-1} h_1^2 + K_{\chi 2}^{-1} h_2^2\right)^{-1}\right] z \\ & \quad + A\left[K_{\varepsilon 2}^{-1} C_7 - K_{\varepsilon 1}^{-1} C_6 - K_{\chi 1}^{-1} h_1 C_{10} - K_{\chi 2}^{-1} h_2 C_{11}\right] z \\ & \quad - [C_3 - A(C_{13} - C_{12} \\ & \quad - h_1 C_{14} - h_2 C_{15}) - B] = 0, \end{aligned} \tag{40}$$

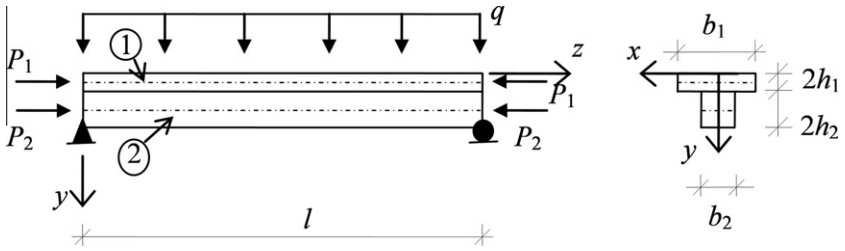

Fig. 4. Two-layer simply supported concrete-wood composite beam (Girhammar and Gopu, 1993).

which is satisfied for any $0 \leqslant z \leqslant L_r$ if and only if:

$$\begin{aligned}
&C_3\left(K_{\varepsilon 1}^{-1}+K_{\varepsilon 2}^{-1}+K_{\chi 1}^{-1}h_1^2+K_{\chi 2}^{-1}h_2^2\right)+K_{\chi 1}^{-1}h_1(m_1-C_8)+K_{\chi 2}^{-1}h_2(m_2-C_9)\\
&\quad+K_{\varepsilon 1}^{-1}q_{z1}-K_{\varepsilon 2}^{-1}q_{z2}=0,\\
&\left(K_{\chi 1}^{-1}h_1q_{y1}+K_{\chi 2}^{-1}h_2q_{y2}\right)\left(K_{\varepsilon 1}^{-1}+K_{\varepsilon 2}^{-1}+K_{\chi 1}^{-1}h_1^2+K_{\chi 2}^{-1}h_2^2\right)^{-1}\\
&\quad+A\left[K_{\varepsilon 2}^{-1}C_7-K_{\varepsilon 1}^{-1}C_6-K_{\chi 1}^{-1}h_1C_{10}-K_{\chi 2}^{-1}h_2C_{11}\right]=0,\\
&C_3-A(C_{13}-C_{12}-h_1C_{14}-h_2C_{15})-B=0.
\end{aligned} \tag{41}$$

In the particular case of $A = 0$, the bond condition (10) reduces to:

$$p_t = B, \tag{42}$$

so that from the first of Eq. (20) it follows:

$$C_3 = 0, \quad C_4 = 0, \quad C_5 = B. \tag{43}$$

To sum up, with reference to the particular two-layer beams satisfying Eq. (15) considered above, the 17 arbitrary constants contained in the general solution of the problem of equilibrium are determined by 5 + 5 = 10 boundary conditions and seven further relations derived by imposing the bond conditions at all points of the interface and given by Eqs. (39) and (41) for $A \neq 0$ or by Eqs. (39) and (43) for $A = 0$.

6. Numerical examples

In this section, firstly, the fundamental closed form solution presented in the previous sections is verified by analyzing case studies already solved by other authors and comparing the results obtained with those found in literature. Secondly, it is shown to be employed in the simulation of the response of composite beams during a loading process inducing a progressive debonding of the interface.

Namely, the bi-linear interface behaviors shown in Fig. 3b are considered here. The imperfect connection in the longitudinal direction is assumed to exhibit firstly an elastic behavior ($A = A_e > 0$, $B = 0$) and then three different post-elastic regimes: (a) a debonded regime ($A = B = 0$), which characterizes brittle interfaces incapable of transmitting any shear traction when the elastic limit is reached, as if the beam consists of two separate layers; (b) a perfectly plastic ($A = 0$, $B = p_e$) or (c) a hardening ($A = A_h > 0$, $B = p_e(1 - A_h/A_e)$) regime, characterizing interfaces capable of transmitting always eventually limited shear tractions when the elastic limit is reached. Three parameters characterize these interface laws: the initial elastic stiffness A_e, the elastic limit shear traction p_e and, only in the case of hardening behavior, the hardening stiffness A_h. A parametric analysis is then performed to investigate which interface parameters have the main influence on the response of composite beams.

The first numerical example refers to a simply supported beam composed of concrete and wood and subjected both to uniformly distributed transverse load and to axial forces, as shown in Fig. 4. This example was considered previously by Girhammar and Gopu (1993) under the assumption of linearly elastic interface. All geometry, material and loading data are summarized in Table 2 together with some significant results; namely, the maximum deflection, shear traction, bending moments and axial forces in each layer at midspan found in literature are compared with those obtained with the analytical solution proposed. An excellent agreement between the two sets of results is observed.

The second numerical example refers to a simply supported beam composed of reinforced concrete (RC) and steel and subjected to uniformly distributed transverse load, as shown in Fig. 5. This example was considered previously by Foraboschi (2009) under the assumption of elasto-perfectly plastic interface. All geometry, material and loading numerical data are summarized in Table 3. In this case, because of the high load level, the interface results to be divided in three portions: the central portion having length l_e undergoes the elastic regime, while the lateral portions having each length $l_p = (l - l_e)/2$ and positioned symmetrically with respect to midspan undergo the perfectly plastic regime (Fig. 5). Some significant results are also shown in Table 3: the length of the elastic portion of the interface, maximum slip at both ends and axial forces in each layer at midspan found in literature are compared with those obtained with the solution presented. A good agreement between the two sets of results in terms of relative error (less than 5% in absolute value) is observed.

As a third numerical example, the two-layer cantilever beam subjected to a load P applied at the free end and shown in Fig. 6 is considered. The two layers have identical constant rectangular

Table 2
Model parameters and significant results for concrete–wood composite beam.

Geometry and material properties	*Interface stiffness and model parameters*
l = 4 m	A_e = 50 MPa
b_1 = 30 cm	$A = A_e$, $B = 0$
$2h_1$ = 5 cm	
b_2 = 5 cm	*Loads*
$2h_2$ = 15 cm	q = 0.01 kN/cm
$K_{\varepsilon 1}$ = 180 MN	P_1 = 37.5 kN
$K_{\chi 1}$ = 375 MN cm^2	P_2 = 12.5 kN
$K_{\varepsilon 2}$ = 60 MN	
$K_{\chi 2}$ = 1125 MN cm^2	

Numerical results at midspan ($z = l/2$)

	Girhammar and Gopu (1993)	Present model
w (mm)	7.56	7.56
p_t (N/m)	11444	11444
N_1 (N)	50863	50862
M_1 (Nm)	165.9	165.9
N_2 (N)	863	862
M_2 (Nm)	497.7	497.8

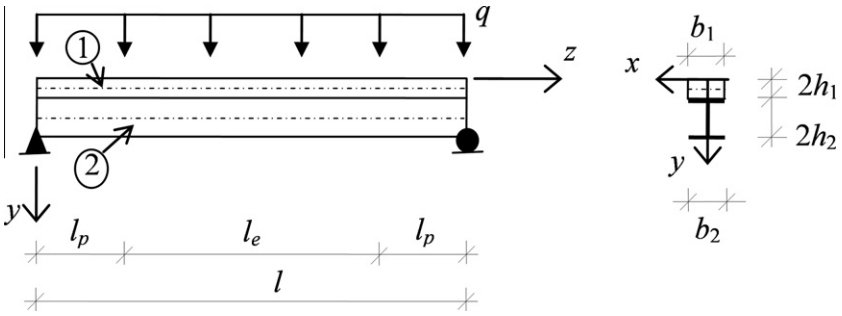

Fig. 5. Two-layer simply supported RC-steel composite beam (Foraboschi, 2009).

Table 3
Model parameters and significant results for concrete-wood composite beam.

Geometry and material properties	*Interface stiffness and model parameters*		
l = 8.20 m	A_e = 1500 MPa		
b_1 = 30 cm	p_e = 2.25 kN/cm		
$2h_1$ = 5 cm			
b_2 = 30cm	*Elastic regime*	*Perfectly plastic regime*	
$2h_2$ = 29cm	$A = A_e, B = 0$	$A = 0, B = p_e$	
$K_{\varepsilon 1}$ = 427.5 MN			
$K_{\chi 1}$ = 890.625 MN cm^2	*Loads*		
$K_{\varepsilon 2}$ = 18270 MN	q = 0.01 kN/cm		
$K_{\chi 2}$ = 1280000 MN cm^2			
Numerical results			
	Foraboschi (2009)	present model	relative error (%)
l_e [cm]	514	536	−4.28
Δs_t [mm] at $z = 0$	0.271	0.279	
Δs_t [mm] at $z = l$	0.271	0.279	
N_1 [kN] at $z = l/2$	600	592	1.33
N_2 [kN] at $z = l/2$	600	592	1.33

cross sections of width b and semi-height h and are made of the same linearly elastic and homogeneous material of Young and tangential moduli E and G, respectively. Geometry and material properties of the beam then satisfy condition (15). The axial, shear and bending stiffnesses of both layers are finally given by:

$$K_{\varepsilon 1} = K_{\varepsilon 2} = K_{\varepsilon} = 2Ebh, \quad K_{\gamma 1} = K_{\gamma 2} = K_{\gamma} = \frac{5}{3}Gbh,$$
$$K_{\chi 1} = K_{\chi 2} = K_{\chi} = \frac{2}{3}Ebh^3. \tag{44}$$

For small loads the whole interface between the layers ($0 \leqslant z \leqslant l$) undergoes only elastic deformation. In this case the problem is linear and its solution straightforward. Normal and shear stresses at the interface are given by Eqs. (18) and (20) for $A > 0$ together with Eqs. (19) and (21), whereas internal forces and displacements follow from Eqs. (35)–(37). The 17 arbitrary constants contained in the general solution are determined by five boundary conditions yielding zero deflection, rotations and axial displacements at the clamped end ($i = 1,2$):

$$w = 0, \quad \varphi_i = 0, \quad u_i = 0 \text{ for } z = 0 \tag{45a}$$

by five boundary conditions yielding resultant shear equal to the applied load and zero bending moments and axial forces at the loaded end ($i = 1,2$):

$$Q = P, \quad M_i = 0, \quad N_i = 0 \qquad \text{for } z = l \tag{45b}$$

and seven further relations given by Eqs. (39) and (41). For the sake of brevity, such a solution is omitted; only some interesting conclusions which can be drawn from the results are discussed. The global stiffness of the composite beam, defined as the ratio between the applied load and the related maximum deflection at the loaded end ($z = l$), say w_{max}, yields:

$$K_e = 320bh^3EGA_e\beta_e[(45EGbh + 96Eh^2A_e + 20Gl^2A_e)\beta_e l - 45EGbh\text{Tanh}[\beta_e l]]^{-1}, \tag{46}$$

where, from Eqs. (21) and (44):

$$\beta_e = 2\sqrt{\frac{A_e}{Ebh}}, \tag{47}$$

and depends on the geometry and material of the beam, as well as on A_e the initial elastic stiffness of the interface between the layers. It is bounded lowerly by the stiffness of a beam composed of two debonded layers (limit case with $A_e \to 0$) and upperly by the stiffness of a beam composed of two perfectly bonded layers (limit case with $A_e \to \infty$). At the interface, no normal tractions act because of symmetry; while shear tractions have the following distribution:

$$p_t = \frac{3P}{8h}\{1 - \text{Cosh}[\beta_e(l - z)]\text{Sech}[\beta_e l]\} \tag{48}$$

with β_e given by Eq. (47), having a maximum absolute value at the loaded end ($z = l$). In Fig. 7 the results obtained for l = 150 cm, b = 12 cm, h = 5 cm, E = 10,000 MPa, G = 500 MPa and different values of A_e = 50, 100, 200 MPa are shown.

When the maximum shear traction at $z = l$ attains the elastic limit value p_e, the post-elastic regime begins. It is reasonable to expect such a process to involve adjacent points and then proceed along the interface towards the clamped end ($z = 0$). The generic configuration of the beam then changes from the one characterized by the whole interface undergoing the elastic behavior to the one

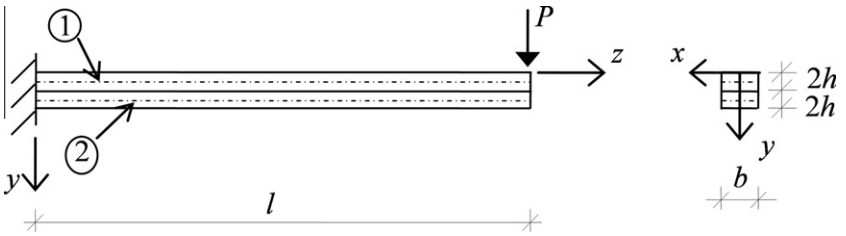

Fig. 6. Two-layer cantilever beam: geometry.

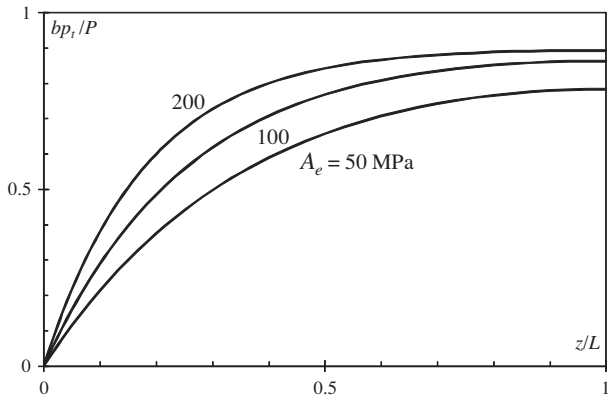

Fig. 7. Two-layer cantilever beam: distribution of interfacial shear tractions for elastic interface with varying interfacial elastic stiffness.

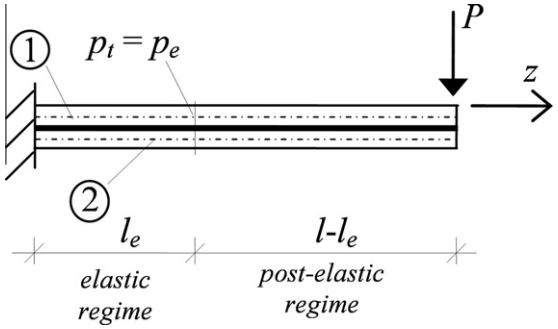

Fig. 8. Two-layer cantilever beam: generic post-elastic configuration.

shown in Fig. 8. In the new configuration the interface is divided in two subdomains: the left portion ($0 \leqslant z \leqslant l_e$) still undergoes the elastic regime, while the right portion undergoes the post-elastic regime ($l_e \leqslant z \leqslant l$). The problem is then nonlinear, since the length l_e of the elastic portion of the interface is unknown a priori. However, because of the irreversibility of the debonding process, l_e decreases monotonically so can be assumed as a non conventional parameter to control this second phase of the loading process in order to catch any branch of the load–maximum deflection curve (including possible snap-through or snap-back branches). On the contrary, the load P can be decreased and so treated as unknown variable of the problem.

With reference to Fig. 8, a generic post-elastic configuration of the beam is considered. Such a generic configuration is geometrically defined by a prescribed value for $l_e < l$ and the related length of the right portion in the post-elastic regime ($l - l_e$). The general solution of the problem then consists of two sets of independent functions for normal and shear interfacial stresses, internal forces and displacements: one set refers to the elastic portion, designated in what follows by subscript "e"; the other refers to the post-elastic portion, designated in what follows by subscript "pe". This general solution then totally contains 34 arbitrary constants. In order to determine them, we have: the following 10 boundary conditions at the clamped and free ends ($i = 1,2$):

$$w_e = 0, \quad \varphi_{ie} = 0, \quad u_{ie} = 0 \qquad \text{for } z = 0 \tag{49a}$$

$$Q_{pe} = P, \quad M_{ipe} = 0, \quad N_{ipe} = 0 \qquad \text{for } z = l; \tag{49b}$$

seven relations given by Eqs. (39) and (41) for the elastic portion; seven relations given by Eqs. (39) and (43) for the post-elastic portion; the following 10 continuity conditions at the boundary between the two portions of the beam:

$$w_e = w_{pe}, \quad \varphi_{ie} = \varphi_{ipe}, \quad u_{ie} = u_{ipe} \qquad \text{for } z = l_e \tag{50a}$$

$$Q_e = Q_{pe}, \quad M_{ie} = M_{ipe}, \quad N_{ie} = N_{ipe} \qquad \text{for } z = l_e. \tag{50b}$$

It is straightforward that this solution depends linearly on the load P which is still unknown. On the other hand, the configuration under consideration is physically compatible if and only if the elastic limit condition at the boundary between the two portions is satisfied:

$$p_{te} = p_{tpe} = p_e \quad \text{for } z = l_e. \tag{51}$$

Solving Eqs. (49)–(51) for C_{je}, C_{jpe} ($j = 1,17$) and P gives the two sets of constants contained in the solution for the elastic and post-elastic portions, respectively, and the value of the load for which the configuration under consideration, corresponding to the prescribed l_e, is equilibrated.

The procedure detailed above has been implemented in an incremental algorithm where at each step the length of the elastic portion is decremented of, say, dl with respect to the length at the previous step until the entire interface undergoes the post-elastic regime ($l_e = 0$). For each step the maximum deflection for $z = l$, say w_{max}, is also calculated.

The mechanical response of the two-layer cantilever beam with interlayer slip and bi-linear interface law is summarized through load–maximum deflection curves, as shown by dimensionless diagrams in Figs. 9–11. A first linear branch describes the initial elastic response of the system according to the global stiffness given by Eq. (46) together with (47). Each point of the subsequent nonlinear branch is related to a specific equilibrated and physically compatible configuration of the beam having a portion of length monotonically decreasing from l to 0 in the elastic interfacial regime and the remaining part of length monotonically increasing from 0 to l exhibiting a post-elastic interfacial regime. It is straightforward that geometry and material properties of both layers and interface strongly affect the response of the composite beam. In this paper, in particular, the effects of the interface parameters are investigated. Figs. 9–11 show the results obtained for $l = 150$ cm, $b = 12$ cm, $h = 5$ cm, $E = 10{,}000$ MPa and $G = 500$ MPa and different values of $A_e = 50$, 100, 200 MPa, $p_e = 1,2,4$ kN/cm and $A_h/A_e = 0.1,0.4$. These results permit several interesting conclusions.

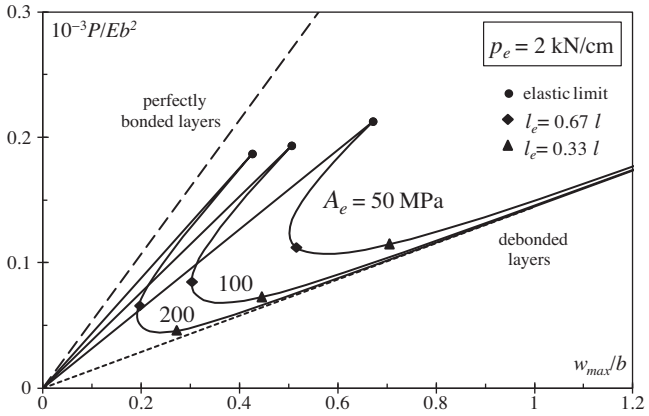

Fig. 9. Two-layer cantilever beam with elastic–brittle interface: load–maximum deflection curves for varying interfacial elastic stiffness.

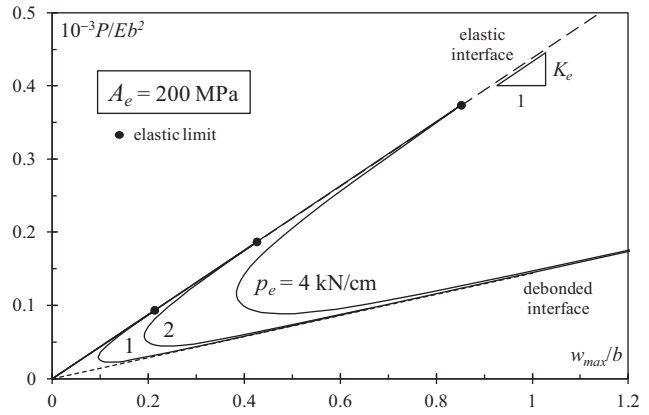

Fig. 10. Two-layer cantilever beams with elastic–brittle interface: load–maximum deflection curves for varying interfacial elastic limit shear traction.

Fig. 9 shows the effects of the initial elastic stiffness A_e of the interface on the global response of the two-layer cantilever beam with elastic–brittle interface in terms of load–maximum deflection curves. This response results to be brittle with a prominent snap-back branch and depends only on A_e. On increasing A_e, the initial global stiffness increases and the response tends to that of a beam composed of two perfectly bonded layers (dashed line), whereas a slight decrease in the strength is produced. A weak influence on the post-elastic response, which always tends to that of a beam composed of two debonded layers (dotted line), is evident. In order to show the decreasing extent of the elastic portion of the interface during the process, the points corresponding to two prescribed configurations with $l_e/l = 0.67$ and 0.33 are marked, in addition to the point representing the elastic limit ($l_e/l = 1$).

Fig. 10 shows the effects of the elastic limit shear traction p_e on the global response of the two-layer cantilever beam with elastic–brittle interface. The response is again brittle and bounded upperly by that induced by a perfectly elastic interface (dashed line) and lowerly by the response of a beam composed of two debonded layers (dotted line). It is evident that the value of p_e affects only the limit of the elastic phase of the global response; in particular, on increasing p_e, the elastic limit load increases.

Finally, the effects of the hardening stiffness A_h of the interface on the global response of the two-layer cantilever beam are shown in Fig. 11 with reference to elastic-hardening interfaces. As expected, A_h affects only the post-elastic response. Once again, we have a first linear elastic branch; whereas the post-elastic response is characterized by a hardening branch. Increasing A_h produces a transition between the lower limit case of the beam with elastic-perfectly plastic interface (dotted line) and the upper limit case of the beam with perfectly elastic interface (dashed line).

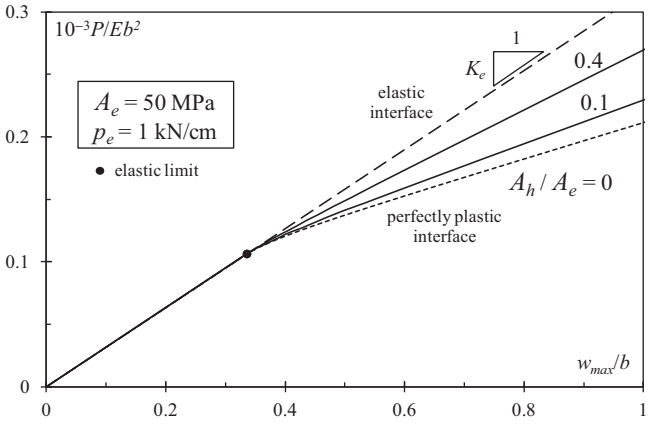

Fig. 11. Two-layer cantilever beams with elastic–hardening interface: load–maximum deflection curves for varying interfacial hardening stiffness.

To conclude, this set of results has been compared with that obtained according to the simplified model, based on Euler–Bernoulli beam theory, discussed in Section 2 and detailed in Appendix A. The comparative analysis of the two sets of results for both static and kinematic variables of the problem has shown only quantitative differences for the deflections and, as a consequence, for the global stiffnesses of the two-layer cantilever beam. In particular, neglecting the effects of shear deformation leads to an overestimate of the global stiffness which is particularly significant in the case of rather stiff connections between the two layers. The percentage error provided by neglecting shear effects (referring to Euler–Bernoulli beam theory rather than Timoshenko beam theory) in the approximation of the global stiffness of the composite beam ranges from about 3% to about 10% depending on the interfacial stiffness. The highest degree of accuracy is obtained for a beam composed of two debonded layers (3% error); the lowest degree of accuracy is found for a beam composed of two perfectly bonded layers (10% error).

7. Conclusions

A novel closed form solution of the problem of two-layer beams with interlayer slip is presented. The layers are modeled as linearly elastic Timoshenko beams; a linear non proportional law relating interfacial shear tractions and slips is chosen to describe the interfacial behavior. Explicit expressions for all static and kinematic variables are derived.

The case study of a two-layer cantilever beam with different bilinear interface laws and subjected to a load at the free end is analyzed and a parametric analysis performed to investigate which interface parameters have the main influence on the response of the composite beam. As expected, in order to optimize the partial composite action in two-layer beams with interlayer slip before the composite system reaches the elastic limit, the joint must present both high elastic stiffness and resistance. Moreover, only an elastic-hardening interface can guarantee a sufficiently ductile subsequent behavior.

Employing the novel closed form solution presented, additional more interesting practical applications involving not only different boundary and loading conditions, but also suitable multi-linear

approximations of nonlinear behaviors for layer materials and/or interface can be also analyzed. However, depending on the complexity of such multi-linear approximations, a more complicated incremental-iterative calculation algorithm than the incremental one described here must be followed and is worth a detailed discussion in a subsequent paper.

Acknowledgements

Support from the University of Genoa and the Italian Ministry of Instruction, University and Research (MIUR), within the Joint Research Projects on "Multiscale mechanical interactions in multilayered materials" and "Multi-scale modelling of materials and structures" (MIUR PRIN09 No. 2009XWLFKW), is gratefully acknowledged.

Appendix A. Simplified fundamental solution according to Euler–Bernoulli beam theory

As noted in Section 2, a simplified formulation based on modeling layers as linearly elastic Euler–Bernoulli beams can be developed as special case of the formulation proposed. The main differences between the two models and related fundamental solutions are discussed here.

According to Euler–Bernoulli beam theory, the shear strains of the two layers ($i = 1,2$) are neglected; from the second of compatibility Eq. (3), then, rotations yield:

$$\varphi_i = -w_i'. \tag{A.1}$$

As a consequence, the connection in the transverse direction being assumed perfect (Eq. (8)), the two layers undergo not only equal deflections w (Eq. (9)) but also equal rotations:

$$\varphi_1 = \varphi_2 = \varphi = -w'. \tag{A.2}$$

Moreover, neglecting shear effects means assuming infinite shear stiffnesses for the layers ($K_{\gamma i} \to \infty$, $i = 1,2$). The equations governing the simplified model can then be straightforwardly derived by setting $K_{\gamma 1}^{-1} = K_{\gamma 2}^{-1} = 0$ in Eqs. (11) and (13). In particular, Eq. (11) is replaced by the following first order differential equation:

$$-\left(K_{\chi 1}^{-1} + K_{\chi 2}^{-1}\right) p_n + \left(K_{\chi 2}^{-1} h_2 - K_{\chi 1}^{-1} h_1\right) p_t' = q_n \tag{A.3}$$

with q_n given by (12); whereas, Eq. (13) remains as it is.

In the case of particular composite beams consisting of two layers having geometry and material properties satisfying the condition (15), Eqs. (A.3) and (13) become uncoupled so their solution is straightforward. In particular, Eq. (A.3) reduces to an algebraic equation whose solution can be written as in Eqs. (18) and (19) having set $C_1 = C_2 = 0$; whereas Eq. (13) reduces to Eq. (17) whose general solution, given by Eqs. (20) and (21), contains three arbitrary constants, say C_j ($j = 3,\ldots,5$).

In the general case of composite beams that do not satisfy condition (15), Eq. (A.3) is first solved for the first derivative of the interfacial shear tractions:

$$p_t' = \left(K_{\chi 1}^{-1} h_1 - K_{\chi 2}^{-1} h_2\right)^{-1} \left[-\left(K_{\chi 1}^{-1} + K_{\chi 2}^{-1}\right) p_n - q_n\right], \tag{A.4}$$

which, substituted in Eq. (13), leads to a second order linear differential equation with constant coefficients for the interfacial normal tractions that can be written as:

$$p_n'' + \hat{b} p_n = \hat{c}, \tag{A.5}$$

where:

$$\hat{b} = -A\left[\left(K_{\varepsilon 1}^{-1} + K_{\varepsilon 2}^{-1}\right) + K_{\chi 1}^{-1} K_{\chi 2}^{-1} \left(K_{\chi 1}^{-1} + K_{\chi 2}^{-1}\right)^{-1} (h_1 + h_2)^2\right], \tag{A.6}$$

$$\hat{c} = \left(K_{\chi 1}^{-1} + K_{\chi 2}^{-1}\right)^{-1} \left[q_t \left(K_{\chi 2}^{-1} h_2 - K_{\chi 1}^{-1} h_1\right) + q_n A \left(K_{\varepsilon 1}^{-1} + K_{\varepsilon 2}^{-1} + K_{\chi 1}^{-1} h_1^2 + K_{\chi 2}^{-1} h_2^2\right)\right], \tag{A.7}$$

with q_n and q_t given by (12) and (14). The general solution of Eq. (A.5) can assume three different forms depending on the interfacial regime:

$$p_n = \begin{cases} C_3 \cosh(\alpha z) + C_4 \sinh(\alpha z) + \bar{p}_n & \text{for } A > 0 \\ C_3 + C_4 z + \hat{c} z^2/2 & \text{for } A = 0 \\ C_3 \cos(\alpha z) + C_4 \sin(\alpha z) + \bar{p}_n & \text{for } A < 0 \end{cases}, \tag{A.8}$$

having defined

$$\alpha = \sqrt{|\hat{b}|} \quad \text{and} \quad \bar{p}_n = \hat{c}/\hat{b}. \tag{A.9}$$

Finally, from integration of Eq. (A.4) the interfacial shear tractions follow and can be written as in Eq. (34) having set $K_{\gamma 1}^{-1} = K_{\gamma 2}^{-1} = 0$.

Analogously to what detailed in Section 4, closed form expressions for all the remaining unknowns (internal forces and displacements) can be derived and assume the forms of Eqs. (35)–(37) having set $K_{\gamma 1}^{-1} = K_{\gamma 2}^{-1} = 0$.

To sum up, the general solution of the problem of equilibrium of two-layer beams with interlayer slip according to the simplified model contains 15 arbitrary constants (C_j with $j = 3,\ldots,17$) to be determined by imposing 15 conditions.

With reference to a segment of composite beam having length L_r, the prescription of boundary conditions at both ends $z = 0$ and $z = L_r$ of the segment gives only 4 + 4 conditions. The kinematic or corresponding static quantities on which such conditions can be imposed are w, φ, u_1, u_2 or, alternatively, $Q = Q_1 + Q_2$, $M = M_1 + M_2$, N_1, N_2. The first boundary condition on w or, alternatively, on the resultant shear Q follows from the assumption of perfect connection in the transverse direction so that the two layers undergo equal deflections. The second boundary condition on φ or, alternatively, on the resultant moment M follows from both the Euler–Bernoulli assumption of negligible shear strain and perfect connection in the transverse direction so that the two layers undergo equal rotations.

Seven additional relations are obtained as detailed in Section 5 for the special case of composite beams having geometry and material properties satisfying Eq. (15). In particular, they are given by Eqs. (39) and (41) for $A \neq 0$ or by Eqs. (39) and (43) for $A = 0$ having set $K_{\gamma 1}^{-1} = K_{\gamma 2}^{-1} = 0$.

References

Adekola, A.O., 1968. Partial interaction between elastically connected elements of a composite beam. Int. J. Solids Struct. 4, 1125–1135.

Bennati, S., Colleluori, M., Corigliano, D., Valvo, P.S., 2009. An enhanced beam-theory model of the asymmetric double cantilever beam (ADCB) test for composite laminates. Compos. Sci. Technol. 69, 1735–1745.

Chajes, M.J., Finch, W.W., Januszka, T.F., Thomson Jr., T.A., 1996. Bond and force transfer of composite material plates bonded to concrete. ACI Struct. J. 93, 208–217.

Cosenza, E., Mazzolani, S., 1993. Analisi in campo lineare di travi composte con connessioni deformabili: formule esatte e risoluzione alle differenze finite. In: Proc. First Italian Workshop on Composite Structures. University of Trento, pp. 1–21 (in Italian).

Foraboschi, P., 2009. Analytical solution of two-layer beam taking into account nonlinear interlayer slip. J. Eng. Mech. 135, 1129–1146.

Gara, F., Ranzi, G., Leoni, G., 2006. Displacement-based formulations for composite beams with longitudinal slip and vertical uplift. Int. J. Numer. Methods Eng. 65, 1197–1220.

Girhammar, U.A., Gopu, V.K.A., 1993. Composite beam-columns with interlayer slip – exact analysis. J. Struct. Eng. 119, 1265–1282.

Girhammar, U.A., Pan, D.H., 2007. Exact static analysis of partially composite beams and beam-columns. Int. J. Mech. Sci. 49, 239–255.

Kroflič, A., Planinc, I., Saje, M., Čas, B., 2010. Analytical solution of two-layer beam including interlayer slip and uplift. Struct. Eng. Mech. 34, 667–683.
Lu, X.Z., Teng, J.G., Ye, L.P., Jiang, J.J., 2005. Bond-slip models for FRP sheets/plates bonded to concrete. Eng. Struct. 27, 920–937.
Manfredi, G., Fabbrocino, G., Cosenza, E., 1999. Modeling of steel–concrete composite beam under negative bending. J. Eng. Mech. 125, 654–662.
McCutcheon, W.J., 1986. Stiffness of framing members with partial composite action. J. Struct. Eng. 112, 1623–1637.
Newmark, N.M., Siess, C.P., Viest, I.M., 1951. Tests and analysis of composite beams with incomplete interaction. Proc. Soc. Exp. Stress Anal. 9, 75–92.
Ollgaard, J.G., Slutter, R.G., Fisher, J.W., 1971. Shear strength of stud connectors in lightweight and normal-weight concrete. AISC Eng. J., 55–64.
Planinc, I., Schnabl, S., Saje, M., Lopatič, J., Čas, B., 2008. Numerical and experimental analysis of timber composite beams with interlayer slip. Eng. Struct. 30, 2959–2969.
Robinson, H., Naraine, K.S., 1988. Slip and uplift effects in composite beams. In: Proceedings of the Engineering Foundation Conference on Composite Construction (ASCE), pp. 487–497.
Schnabl, S., Saje, M., Turk, G., Planinc, I., 2007. Analytical solution of two-layer beam taking into account interlayer slip and shear deformation. J. Struct. Eng. 133, 886–894.
Schreyer, H.L., Peffer, A., 2000. Fiber pullout based on a one-dimensional model of decohesion. Mech. Mater. 32, 821–836.
Wang, J., Qiao, P., 2004. Interface crack between two shear deformable elastic layers. J. Mech. Phys. Solids 52, 891–905.
Wang, J., 2006. Debonding of FRP-plated reinforced concrete beam, a bond-slip analysis. I. Theoretical formulation. Int. J. Solids Struct. 43, 6649–6664.
Wheat, D.L., Calixto, J.M., 1994. Nonlinear analysis of two-layered wood members with interlayer slip. J. Struct. Eng. 120, 1909–1929.
Xu, R., Wu, Y., 2007. Static, dynamic and buckling analysis of partial interaction composite members using Timoshenko's beam theory. Int. J. Mech. Sci. 49, 1139–1155.